Journal of Computers Vol. 28, No. 4, 2017, pp. 148-156
doi:10.3966/199115592017082804016

# DC-Link Stability Analysis for AC Drive System with Common DC-Bus

Xiaoyan Wen

Beijing Key Laboratory of Robot Bionics and Function Research, Beijing University of Civil Engineering and Architecture, 100044, Beijing, China
wenxiaoyan@bucea.edu.cn

Received 25 October 2016; Revised 13 June 2017; Accepted 26 June 2017

**Abstract**. AC drive system with common DC-bus is widely used in industry process, however, because of inductance in rectifier and negative resistance characteristic of inverter-motor system, DC-bus fluctuation often appears. With small signal method and power-fed AC drive test-bed, this paper studies stability of AC drive system with common DC-bus. First, structure of AC drive system with common DC-bus and power-fed test-bed are introduced, and its small signal mathematic model is derived. Then, stability of test-bed is studied from the point of DC-link stability, and system parameter and operation point effect on stability is also discussed. Beyond that, system stability area is compared with ordinary AC drive system. The conclusion shows that common DC-bus system has a priority than ordinary AC drive system without power-fed structure in the view of DC-bus stability. Experiment results validate above analysis conclusions. What's more, the conclusion provides an advice for drive system parameter choice.

**Keywords**: AC drive system, common DC-bus, DC-link stability, power-fed test-bed, small signal method

## 1 Introduction

As the development of full controlled power electronic device and relative control theory, AC drive technology has been mature and AC drive system supplied by voltage source converter (VSC) is more and more widely used [1-2]. For energy saving, common DC-bus is popular in AC drive system, while DC-bus voltage fluctuation often shows up in AC drive system because of inductance in converter main circuit and negative resistance characteristic of inverter-motor system.

DC-bus stability problem of AC drive system has been concerned for a long time [1, 3-18], and there are several typical methods used to analyze this issue. A lot of researchers use equivalent circuit method. For instance, according to DC side characteristic of VSC-motor system, Sudhoff, Corzine and Glover treats them as a current source, and analyzes DC-bus stability using small signal analysis method [3]. By assuming motor rotational speed changing slowly, Marx, Pierfederici and Davat makes the same conclusion with Sudhoff et al. by treating VSC-motor as a constant power load [3-4]. Zhang and Li uses series connection of resistance and electromotive force as the equivalence of VSC-motor system [5]. While some researchers like to convert DC-bus impedance to AC side of inverter and combining it with motor model [6-8]. Some researchers tend to analyze this problem from the view of motor parameter. For example, with motor model under two-phase synchronous rotating frame, Shen derives its impedance, calculates DC side equivalent value and analyzes motor parameter effect on system stability [9]. While, Fallside and Patel uses Lyapunov function to analyze AC drive system stability [10]. Instead of requiring definite Lyapunov function (V), Fallside and Patel determine stability area by judging definite area of V or its differentiation dV [10]. To eliminate the un-stability, many theories has been used. Instability problem shows up in AC drive system where VSC is supplied by PWM converter, so DC-bus voltage is controlled by power balance theory and input/output feedback linearization to eliminate motor load influence on DC-bus voltage [11]. While Machado, Trovao and Antunes solves this with Kalman filter [12]. This issue has been studied for so long time, but it is still a tough problem, and it involves more

application area, where micro-grid system is included [15-18], so this problem should be solved well soon.

Although lots of research has been done in above literatures, they usually do the research with ordinary AC drive system, where inverters are usually powered separately. This paper studies DC-bus stability of power-fed AC drive system in which there are two inverter-motor systems and a common DC-bus is shared by these two inverters. This structure is widely used in industrial process now mentioned ahead.

## 2 System Structure and Mathematic Model

### 2.1 System Structure

Generally speaking, common DC-bus AC drive system contains four kinds of components: converter, inverter-motor, capacitance and energy storing/feedback device. Its diagram is shown in Fig. 1 [1].

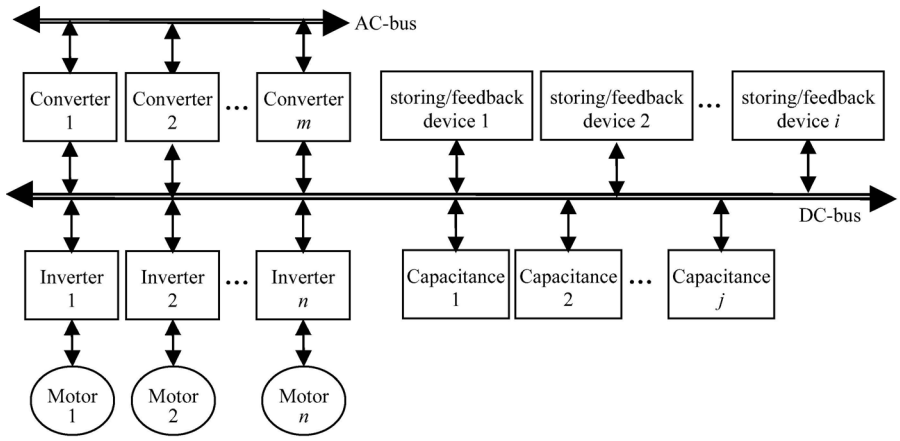


**Fig. 1.** Diagram of common DC-bus AC drive system

For generalization, in Fig. 1, quantities of converter, inverter-motor, energy storing/feedback device and motor are *m*, *n*, *i* and *j*. For power-fed AC drive test-bed discussed in this paper, *m*=1, *n*=2, *i*=0, and *j*=1. And its structure is shown in Fig. 2.

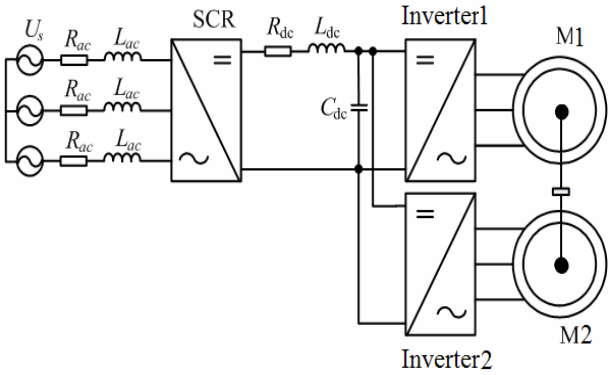


**Fig. 2.** Power-fed test-bed system structure

As is shown in Fig. 2, the power-fed test-bed system adopts silicon controlled rectifier (SCR) as converter, DC side of two inverters (Inverter1 and Inverter2) are connected together (called common DC-bus), and two motors (M1 and M2) are coupled with shaft. Because of system structure, Inverter1-M1 and Inverter2-M2 are role equivalent. During operation, usually one motor works as drive motor and takes closed loop rotational speed control (generally M1), and the other works as load modeling and takes torque as controlled variable (generally M2).Of course, these two motors can work with other controlled variable combination, for instance, M1 and M2 take torque and speed control separately.

Parameters implication in Fig. 2 is as following:

$U_s$: AC voltage RMS value;
$R_{ac}$: AC-side resistance of SCR;
$L_{ac}$: AC-side inductance of SCR;
$R_{dc}$: DC-bus resistance;
$L_{dc}$: DC-bus inductance;
$C_{dc}$: DC-bus capacitance.

### 2.2 Mathematic Model of Test-bed System

When power-fed test-bed works at steady state, assume DC-bus voltage is $U_{dc}$, trigger angle of SCR is$\alpha$, rotational speed of shaft is $n$(r/min), load torque simulated is $T_m$(Nm), power flowing into Inverter1 and Inverter2 are $P_1$ and $P_2$, and efficiencies of M1 and M2 are $\eta_1$ and $\eta_2$ respectively.

Ignoring inverter power loss, inverter-motor system could be treated as a controlled current source according to power balance law. What's more, AC side resistance and inductance of SCR can be converted to DC side with equivalent parameters [3]. With this operation, equivalent circuit of test-bed can be derived and is shown in Fig. 3.

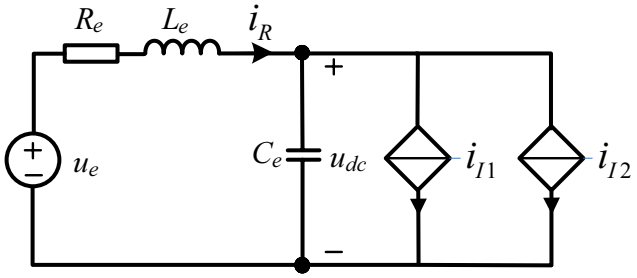


**Fig. 3.** Equivalent circuit of power-fed AC drive test-bed

In Fig. 3, parameters implication is as following:
$u_e$: equivalent DC source voltage for AC source;
$R_e$: equivalent DC resistance of DC-bus and SCR;
$L_e$: equivalent DC inductance of DC-bus and SCR;
$C_e$: equivalent DC capacitance of DC-bus and SCR;
$i_R$: DC-bus current provided by SCR;
$i_{I1}$: equivalent controlled current source for Inverter1-motor1;
$i_{I2}$: equivalent controlled current source for Inverter2-motor2.
Parameter values and relationships among above them are [0]:

$$u_e = \frac{3\sqrt{6}}{\pi} U_s \cos(\alpha) \tag{1}$$

$$R_e = 2R_{ac} + R_{dc} + \frac{3\omega L_{ac}}{\pi} \tag{2}$$

$$L_e = L_{dc} \tag{3}$$

$$i_{I1} = P_1/u_{dc} \tag{4}$$

$$i_{I2} = P_2/u_{dc} \tag{5}$$

According to Fig. 3, equation (4) and (5), state equation of power-fed test-bed equivalent circuit is obtained:

$$\begin{bmatrix} \frac{di_{\mathrm{R}}}{dt} \\ \frac{du_{\mathrm{dc}}}{dt} \end{bmatrix} = \begin{bmatrix} -\frac{R_{\mathrm{e}}}{L_{\mathrm{e}}} & -\frac{1}{L_{\mathrm{e}}} \\ \frac{1}{C_{\mathrm{e}}} & -\frac{1}{C_{\mathrm{e}}}\frac{P_1+P_2}{u_{dc}^2} \end{bmatrix} \begin{bmatrix} i_R \\ u_{dc} \end{bmatrix} + \begin{bmatrix} \frac{1}{L_e} \\ 0 \end{bmatrix} u_{\mathrm{e}} \tag{6}$$

Considering small displacement around operating point, and assume displacements of DC-bus voltage and DC currents flowing into inverters are $\Delta u_{\mathrm{dc}}$, $\Delta i_{\mathrm{I1}}$ and $\Delta i_{\mathrm{I2}}$, we have:

$$\Delta i_{\mathrm{I1}} = -\frac{P_1}{u_{\mathrm{dc}}^2}\Delta u_{\mathrm{dc}}$$

$$\Delta i_{\mathrm{I2}} = -\frac{P_2}{u_{\mathrm{dc}}^2}\Delta u_{\mathrm{dc}}$$

So small-signal mathematic model for power-fed test-bed is derived:

$$\begin{bmatrix} \frac{d\Delta i_R}{dt} \\ \frac{d\Delta u_{dc}}{dt} \end{bmatrix} = \begin{bmatrix} -\frac{R_e}{L_e} & -\frac{1}{L_e} \\ \frac{1}{C_e} & -\frac{P_1+P_2}{C_e u_{dc}^2} \end{bmatrix} \begin{bmatrix} \Delta i_R \\ \Delta u_{dc} \end{bmatrix} + \begin{bmatrix} \frac{1}{L_e} \\ 0 \end{bmatrix} \Delta u_e \tag{7}$$

## 3 DC-bus Stability Analysis

### 3.1 DC-Bus Voltage Stability Constraint Condition

According to equation (7), characteristic equation of small-signal model is:

$$\lambda^2 + \left(\frac{R_{\mathrm{e}}}{L_{\mathrm{e}}} - \frac{1}{C_{\mathrm{e}}}\frac{P_1+P_2}{u_{dc}^2}\right)\lambda + \frac{1}{L_{\mathrm{e}}C_{\mathrm{e}}}\left(1 - \frac{R_e\left(P_1+P_2\right)}{u_{dc}^2}\right) = 0 \tag{8}$$

In (8), λ is characteristic value of the equation.

On the basis of Routh stability criteria, if the system is stable, then λ and relative parameter should satisfy the following constraint condition:

$$\begin{cases} R_e > \dfrac{L_e}{C_e}\dfrac{P_1+P_2}{u_{dc}^2} & (a) \\ R_e < \dfrac{u_{dc}^2}{P_1+P_2} & (b) \end{cases} \tag{9}$$

### 3.2 System Operation Point's Effect

From equation (9), how system parameters ($R_{\mathrm{e}}$, $L_{\mathrm{e}}$, $C_{\mathrm{e}}$) and operation point ($u_{\mathrm{dc}}$, $P_1$, $P_2$) influence DC-bus stability can be demonstrated in the way of Table 1. In Table 1, "+" stands for "the bigger the parameter is, the more stable the system is", while "-" stands for 'the smaller the parameter is, the more stable the system is'.

**Table 1.** System parameter and operation point effect on stability

| Parameter/operation point | $R_{\mathrm{e}}$ | $L_{\mathrm{e}}$ | $C_{\mathrm{e}}$ | $u_{\mathrm{dc}}$ | $P_1+P_2$ |
|---|---|---|---|---|---|
| Effect on system stability | + | - | + | + | - |

From Table 1, system parameters ($R_{\mathrm{e}}$, $L_{\mathrm{e}}$, $C_{\mathrm{e}}$) and $u_{\mathrm{dc}}$ effect on DC-bus stability is obvious. But, for $P_1$ and $P_2$, it needs more specific discussion at different operation point.

Considering Inverter1-M1 and Inverter2-M2 have the same parameter, and their functions are

symmetrical, in the following, it is under this supposition: M1 works as a drive motor and M2 works as a load emulator, that is to say, M2 works as a generator. Thus, DC power flowing into Inverter1 is always positive ($P_1$>0); while, with consideration of M2 power loss, the sign of $P_2$ is not definite, and it is determined by system operation point.

**Effect of rotational speed.** In order to confirm sign of $P_2$, motor power loss and mechanical power input of M2 should be compared. As a popular and widely used control strategy, vector control is used in test-bed system. With vector control, stator current can be decomposed into two components: flux current and torque current, and these two components determine motor power loss together. For operation point under nominal frequency, flux current is generally a constant, so power loss has positive correlation with torque current, while torque current component is in scale to torque load.

If torque load is the same, for a higher rotational speed, mechanical power input to M2 is bigger, while there is no obvious change for its power loss. So, for higher speed, mechanical power input is more likely bigger than motor power loss, and M2is more likely works as a generator, and send power to DC-bus through Inverter2, that is to say $P_2 < 0$. At this condition, (9) is much easier to satisfy, in other words, the system is much more stable.

While, under same torque load, when rotational speed is very small, there could be a condition: M2 works as a generator, but mechanical power input to M2 is smaller than its power loss, and M2 absorbs power from DC-bus ($P_2$>0) in fact. Then, (9) is difficult to satisfy, in other words, the system is less stable.

From above discussion, at same $R_e$, $L_e$, $C_e$, $u_{dc}$ and torque load, higher speed point is more stable than low speed point.

**Effect of torque load.** Similarly, for same rotational speed, when torque load is small, power loss of M2 is small, M2 would output power to DC-bus, that is to say $P_2$<0, and system is much easier to be stable. If the torque load is heavy, power loss of M2 would be large, and the condition of $P_2$>0 appears, then system would be less stable.

From the above, at same $R_e$, $L_e$, $C_e$, $u_{dc}$ and rotational speed, small load emulation is more stable than heavy load. System operation point effect on DC-Link stability is clear. The same conclusion will be derived if M1 and M2 switch their role.

### 3.3 Stability Comparison of Common DC-bus AC Drive System and Ordinary One

For ordinary AC drive system, it can be treat as a special condition of AC drive system with common DC-bus, and its stable constraint condition can be derived with the same method for power-fed test-bed by considering $P_2$ =0, which is in detail:

$$\begin{cases} R_e > \dfrac{L_e}{C_e}\dfrac{P_1}{u_{dc}^2} \\ R_e < \dfrac{u_{dc}^2}{P_1} \end{cases} \tag{10}$$

Assuming a common DC-bus AC drive system and an ordinary one have the same system parameter($R_e$, $L_e$, $C_e$), and two kinds of system work at a same operation point ($u_{dc}$, rotational speed and torque load), then equation (9) is easier to satisfy than equation (10) when the rotational speed is high enough and torque load is light enough to make $P_2 < 0$, because we have equation (11) under this condition:

$$\begin{cases} \dfrac{L_e}{C_e}\dfrac{P_1+P_2}{u_{dc}^2} < \dfrac{L_e}{C_e}\dfrac{P_1}{u_{dc}^2} < R_e \\ R_e < \dfrac{u_{dc}^2}{P_1} < \dfrac{u_{dc}^2}{P_1+P_2} \end{cases} \tag{11}$$

There is a possibility that AC drive system with common DC-bus is less stable than ordinary one, and this occurs only if rotational speed is too small and torque load is very heavy at the same time, which would lead to$P_2 > 0$. But this kind of operation mode takes a very small ratio.

So we can have a corollary: generally speaking, AC drive system with common DC-bus is much more

stable than ordinary one.

## 4 Experiment Results

To validate above analysis conclusion, comparison experiments is taken on an AC drive system with common DC-bus: power-fed AC drive test-bed. During experiment, M1 and M2 adopt general operation mode: M1 works as drive motor, and M2 works as load emulator. In the following results, $u_{dc}$ stands for DC-bus voltage, Fr is rotor frequency, $T_m$ is torque load emulated and $i_a$ is phase-A current of M1.Because Fr equals shaft rotation frequency multiply pole pairs, so Fr stands for rotational speed.

### 4.1 Effect of Rotational Speed

If two operation points take same $u_{dc}$ and $T_m$, then the higher speed operation point would be more stable. Results showed in Fig. 4 and Fig. 5 prove this conclusion.

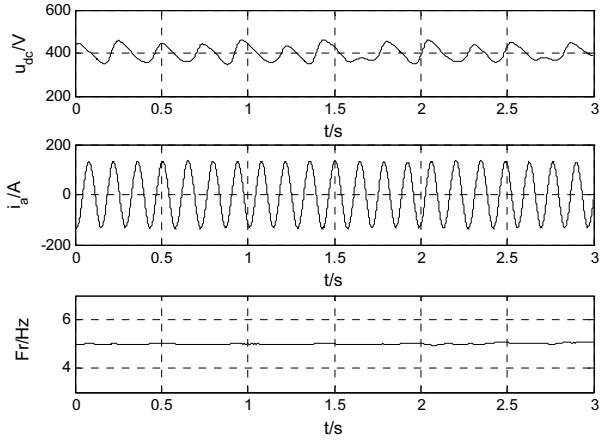


**Fig. 4.** $u_{dc}$ = 400V, Fr = 5Hz, $T_m$ = 480Nm

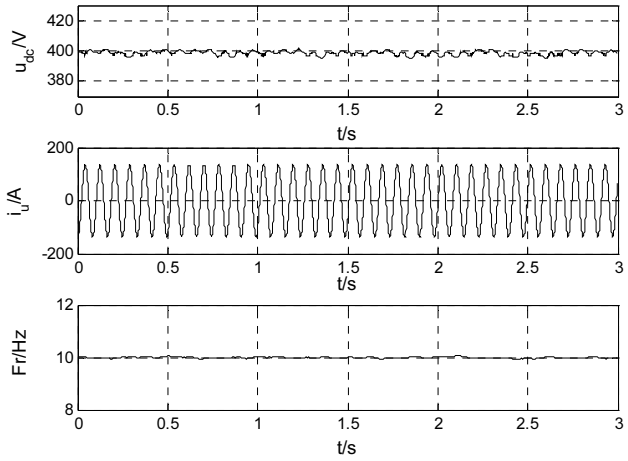


**Fig. 5.** $u_{dc}$ = 400V, Fr = 10Hz, $T_m$ = 480Nm

For results in Fig. 4, system operation condition is: $u_{dc}$ =400V, Fr=5Hz, $T_m$=480Nm. As is shown, DC-bus voltage fluctuation appears, and its wave range is about 100V.

When increasing Fr to 10Hz and keeping other operation condition, experiment result is shown in Fig. 5. Obviously, in Fig. 5, DC-bus voltage fluctuation decreases a lot, and its wave range is less than 5V.

During above two experiments, the controllers have been well tuned. So in both Fig. 4 and Fig. 5, Fr is well controlled, and motor current is also steady and have good waveform. With all the same condition except rotational speed, $u_{dc}$ appears very differently and the difference is coincident with analysis

conclusion.

### 4.2 Effect of Torque Load

When $u_{dc}$ and Fr are the same, heavy load operation point would be less stable.

For results in Fig. 6, system operation condition is: $u_{dc}$ = 400V, Fr = 5Hz, $T_m$ = 360Nm. As is shown in Fig. 6, DC-bus voltage fluctuation is very small, and wave range is less than 5V.

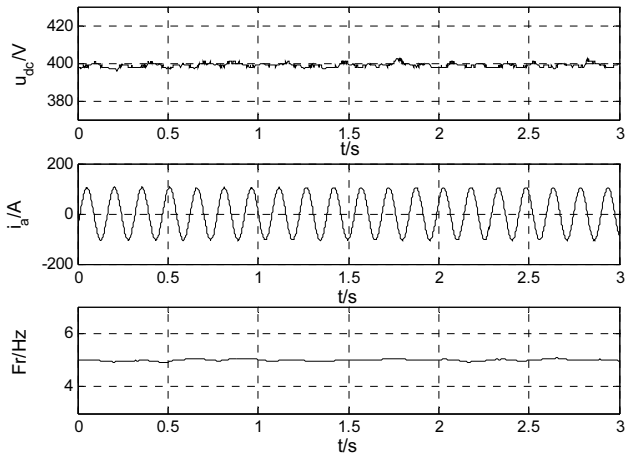


**Fig. 6.** $u_{dc}$ = 400V, Fr = 5Hz, $T_m$ = 360Nm

Compare Fig. 4 and Fig. 6 and their operation conditions, the analysis conclusion is validated.

### 4.3 Effect of DC-bus Voltage

Increase $u_{dc}$ to 600V while keeping other conditions the same with Fig. 4, result in Fig. 7 is observed. By comparing Fig. 4 and Fig. 7, effect of $u_{dc}$ on system stability is derived and it is coincident with former conclusion in section 3.2.

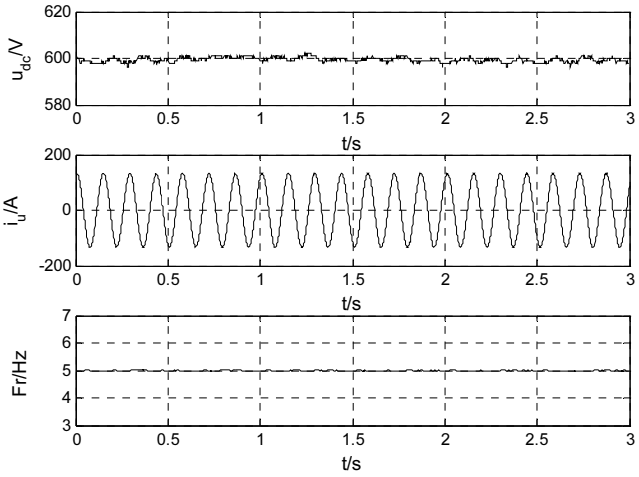


**Fig. 7.** $u_{dc}$ = 600V, Fr = 5Hz, $T_m$ = 480Nm

## 5 Conclusion

This paper analyzes DC-link stability of AC drive system with common DC-bus and validates relative conclusions by experiments on power-fed AC drive test-bed. After demonstrating general structure of AC drive system with common DC-bus, this paper introduces power-fed test-bed, and derives its small signal mathematic model. In this model, inverter-motor is treated as a controlled current source and AC side components of SCR are converted to their DC side equivalent parameter. Then, from mathematic model

characteristic equation, DC-link stability constraint condition is derived, on the basis of that, system parameters and operation point effect on stability are analyzed and derives several conclusions: (1) if other conditions are the same, high speed area is more stable than low speed, (2) if other conditions are the same, light load is beneficial to stability, (3) if other conditions are the same, high DC-bus voltage is good to system stability, (4) comparing with ordinary one, AC drive system with common DC-bus has its advantage in stability expect special operation condition: rotational speed is very low and torque load is very heavy at the same time. Besides, the conclusion could be useful for system parameter choosing.

## Acknowledgement

This work is supported by Beijing Key Laboratory of Robot Bionics and Function ResearchFound (Number: 07080915001).

## References

[1] J. Li, T. Tang, G. Yao, Modeling and analysis for common DC bus AC drive energy-saving system based on hybrid systems, in: Proc. Transactions of China Electrotechnical Society, 2011.

[2] D. Xie, J. Feng, Y. Lou, M. Yang, X. Wang, Small-signal modeling and modal analysis of DFIG-based wind turbine based on three-mass shaft model, in: Proc. the CSEE, 2013.

[3] S.D. Sudhoff, K.A. Corzine, S.F. Glover, DC link stabilized field oriented control of electric propulsion systems, IEEE Transactions on Energy Conversion 13(1)(1998) 27-33.

[4] D. Marx, S. Pierfederici, B. Davat, Nonlinear control of an inverter motor drive system with input filter-large signal analysis of the DC-Link voltage stability, in: Proc. IEEE Power Electronics Specialists Conference, 2008.

[5] J. Zhang, H. Li, X. Feng, Research on load equivalent model of four-quadrant converters, Transactions of China Electrotechnical Society 23(1)(2008) 72-76.

[6] R.H. Nelson, T.A. Lipo, P.C. Krause, Stability analysis of a symmetrical induction machine, IEEE Transactionson Power Apparatus and Systems PAS-88(11)(1969) 1710-1717.

[7] T.A. Lipo, P.C. Krause, Stability analysis of a rectifier-inverter induction motor drive, IEEE Transactions on Power Apparatus and Systems PAS-88(1)(1969) 55-66.

[8] T. Summers, R.E. Betz, Stability analysis of the instantaneous power control(IPC) algorithm for induction machines, in: Proc. European Conference on power electronics and applications, 2007.

[9] J. Shen, Inverter drive system stability for traction applications, in: Proc. 2005 IEEE Vehicle Power and Propulsion Conference(VPPC), 2005.

[10] F. Fallside, M.R. Patel, Estimating regions of a symptotic stability using non-sign-definite Lyapunov functions, in: Proc. Electronics Letters, 1965.

[11] P. Liutanakul, S. Pierfederici, F. Meibody-Tabar, Nonlinear control techniques of a controllable rectifier/inverter-motor drive system with a small dc-link capacitor, Energy Conversion and Management 49(12)(2008) 3541-3549.

[12] F. Machado, J.P. Trovao, C.H. Antunes, DC-link stability control for dual-source electric vehicles using an extended kalman filter, in: Proc. 39th Annual Conference of the IEEE Industrial Electronics Society, 2013.

[13] H.A. Peterson, P.C. Krause, A direct- and quadrature-axis representation of a parallel AC and DC power system, IEEE Transactions on Power Apparatus and Systems, PAS-85(3)(1966) 210-225.

[14] W. Chen, R. Yang, Y. Yu, Z. Xu, D. Xu, Novel stability improvement method for V/F controlled induction motor drive

systems, Electric Machines and Control S1(2009) 45-49.

[15] Y. Huang, D. Wang, Modeling and stability analysis of DC-Link voltage control in multi VSCs with integrated to weak grid, IEEE Transactions on Energy Conversion PP(99)(2017) 1-1.

[16] S. Madhusoodhanan, A. Tripathi, D. Patel, K. Mainali, S. Bhattacharya, Stability analysis of the high voltage DC link between the FEC and DC-DC stage of a transformer-less intelligent power substation, in: Proc. IEEE Energy Conversion Congress and Exposition (ECCE), 2014.

[17] Y. Huang, X. Zhai, J. Hu, D. Liu, C. Lin, Modeling and stability analysis of VSC internal voltage in DC-Link voltage control time scale, IEEE Journal of Emerging and Selected Topics in Power Electronics PP(99)(2017) 1-1.

[18] M. Nikouie, O. Wallmark, L. Jin, L. Harnefors, H.P. Nee, DC-Link stability analysis and controller design for the stacked polyphase bridges converter, IEEE Transactions on Power Electronics 32(2)(2017) 1666-1674.